Indian Journal of Chemistry
Vol. 50A, March-April 2011, pp. 519-530

# Photocytotoxicity and DNA photocleavage activity of La(III) and Gd(III) complexes of phenanthroline bases

Akhtar Hussain[a], Sounik Saha[a], Ritankar Majumdar[b], Rajan R Dighe[b] & Akhil R Chakravarty[a,*]

[a]Department of Inorganic and Physical Chemistry, Indian Institute of Science, Bangalore 560 012, India

Email: arc@ipc.iisc.ernet.in

[b]Department of Molecular Reproduction, Development and Genetics, Indian Institute of Science, Bangalore 560 012, India

*Received 1 October 2010; accepted 20 January 2011*

Lanthanide(III) complexes $[La(B)(acac)_3]$ (**1**–**3**) and $[Gd(B)(acac)_3]$ (**4**–**6**), where B is a *N,N*-donor phenanthroline base, viz., 1,10-phenanthroline (phen in **1**, **4**), dipyrido[3,2-*d*:2′,3′-*f*]quinoxaline (dpq in **2**, **5**) and dipyrido[3,2-*a*:2′,3′-*c*]phenazine (dppz in **3**, **6**), have been prepared and characterized. The Gd(III) complexes **4** – **6** are structurally characterized by single crystal X-ray crystallography. The complexes display $GdO_6N_2$ coordination with the ligands showing bidentate chelating mode of bonding. The complexes are non-electrolytic in aqueous DMF and exhibit ligand-centered absorption bands in the UV region. The dppz complexes show a band at 380 nm in DMF. The La(III) complexes are diamagnetic. The Gd(III) complexes are paramagnetic with magnetic moment that corresponds to seven unpaired electrons. The complexes are avid binders to calf thymus DNA giving $K_b$ values in the range of $4.7 \times 10^4 - 6.1 \times 10^5$ $M^{-1}$ with a relative binding order: **3**, **6** (dppz) > **2**, **5** (dpq) > **1**, **4** (phen). The binding data suggest DNA surface and/or groove binding nature of the complexes. The dpq and dppz complexes efficiently cleave SC DNA to its nicked circular form in UV-A light of 365 nm via formation of both singlet oxygen ($^1O_2$) and hydroxyl radical ($HO^\bullet$) species. The dppz complexes **3** and **6** exhibit significant PDT effect in HeLa cervical cancer cells giving respective $IC_{50}$ value of 460(±50) and 530(±30) n$M$ in UV-A light of 365 nm, and are essentially non-toxic in dark with an $IC_{50}$ value of >100 μ$M$. The dppz ligand alone is cytotoxic in dark and UV-A light. A significant decrease in the dark toxicity of the dppz base is observed on binding to the Ln(III) ion while retaining its photocytotoxicity.

**Keywords:** Bioinorganic chemistry, Lanthanides, Phenanthroline bases, Crystal structures, DNA binding, DNA photocleavage, Photocleavage, Photocytotoxicity, Cytotoxicity

Metal-based photodynamic therapeutic (PDT) agents are of considerable current interests for their potential applications as viable alternatives to the organic-based PDT agents for cancer cure and management[1-12]. Organic PDT agents such as porphyrins and phthalocyanines show photocytotoxicity on generation of cytotoxic singlet oxygen as an active species in a type-II pathway and the efficacy of these PDT agents depends on the quantum yield of singlet oxygen generation[13]. Metal-based PDT agents, in contrast, could undergo type-I and/or photo-redox pathways in addition to the type-II process[14]. Recent reports have shown that platinum(IV), ruthenium(II) and rhodium(II) complexes could be suitably designed to observe photocytotoxicity in a variety of cancer cell lines[1-8]. The reports from our group have shown that iron(III) and oxovanadium(IV) complexes are potential 3*d* metal-based PDT agents exhibiting significant light-induced photocytotoxicity[9,10]. The present work stems from our interest to develop the chemistry of lanthanide(III) complexes as potent PDT agents. Lanthanide(III) complexes with their varied coordination geometries and high coordination number could be suitably designed using organic photosensitizers to achieve efficient oxidative DNA cleavage activity and reduced hydrolytic cleavage activity. In addition, the low dark toxicity of the lanthanide(III) complexes is due to redox stability of the metal thus making lanthanide complexes suitable for cellular applications in the presence of reducing cellular thiols. Besides, the photo-induced DNA cleavage activity of lanthanide complexes is relatively unexplored[15-19]. Lutetium(III) texaphyrin (LUTRIN®) has been successfully used as a PDT agent[15]. Other medicinal applications of lanthanides include gadolinium(III) complexes such as $[Gd(DTPA)(H_2O)]^{2-}$

(Magnevist™) and $[Gd(DOTA)(H_2O)]^-$ (Dotarem™) that are currently used clinically as Magnetic Resonance Imaging (MRI) contrast agents[20-22].

We have recently reported La(III) and Gd(III) complexes of phenanthroline bases (B), viz., $[LnB_2(NO_3)_3]$ as photo-induced DNA cleaving agents and the dppz complexes are found to show photocytotoxicity in HeLa cells[18] in UV-A light of 365 nm. It has been observed that the complexes show structural changes on dissolution due to dissociation of the nitrate ligand. A major drawback of the bis-complexes is the *cis*-disposition of two phenanthroline bases making the complexes structurally unsuitable towards effectively binding the DNA structure. To ensure better solution stability of the complexes and better DNA binding efficacy, we have used acetylacetonate anion instead of nitrate and the very presence of three acac ligands makes one phenanthroline base binding to the Ln(III) instead of two such bases. Herein, we report the synthesis, characterization, DNA binding and cleavage, and photocytotoxicity of the lanthanide(III) complexes $[La(B)(acac)_3]$ (**1–3**) and $[Gd(B)(acac)_3]$ (**4–6**), where B is a *N,N*-donor phenanthroline base, viz., 1,10-phenanthroline (phen in **1, 4**), dipyrido-[3,2-*d*:2′,3′-*f*]quinoxaline (dpq in **2, 5**), dipyrido-[3,2-*a*:2′,3′-*c*]phenazine (dppz in **3, 6**), and acac is acetylacetonate (Fig. 1). Complexes **4**-**6** have been structurally characterized by X-ray crystallography. We have used dpq and dppz as photo-active planar phenanthroline bases since such ligands are known to generate photo-excited $^3(n\text{-}\pi^*)$ and/or $^3(\pi\text{-}\pi^*)$ state cleaving DNA on photo-irradiation with high energy UV light[23]. The significant result of this study is the PDT effect of the dppz complexes in HeLa cancer cells in UV-A light of 365 nm, while the complexes remain essentially non-toxic in the dark. The structure-activity relationship (SAR) shows the photocytotoxicity of the mono-dppz complexes being similar to those of the reported bis-dppz complexes, possibly due to the solution structural differences between two series of lanthanide(III) dipyrido-phenazine complexes[18]. The crystal structure of complex **6** is of importance since structurally characterized Ln(III) complexes of the biologically active dppz ligand is presently unknown in the literature.

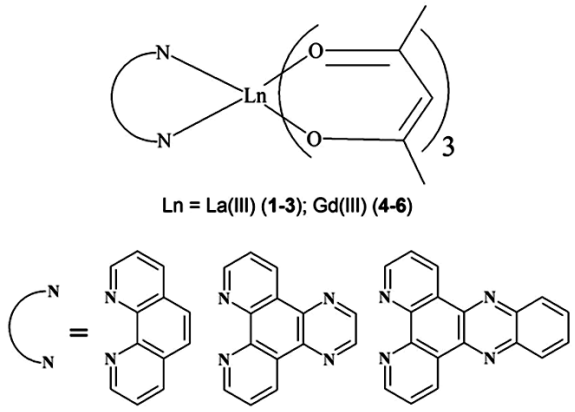


Fig. 1 – Complexes **1**–**6** and the phenanthroline bases used.

## Materials and Methods

All the reagents, lanthanide salts and chemicals were procured from commercial sources (SD Fine Chemicals, India; Aldrich, USA) and used without any further purification. Solvents used were purified by standard procedures[24]. Supercoiled (SC) pUC19 DNA (cesium chloride purified) was from Bangalore Genie (India). Calf thymus (CT) DNA, agarose (molecular biology grade), distamycin-A, methyl green, catalase, superoxide dismutase (SOD), 2,2,6,6-tetramethyl-4-piperidone (TEMP), 1,4-diaza-bicyclo[2.2.2]octan (DABCO), ethidium bromide (EB) and Hoechst 33258 were from Sigma, USA. Tris-(hydroxymethyl)aminomethane-HCl (Tris-HCl) buffer solution was prepared using deionized and sonicated triple distilled water using a quartz water distillation setup. The *N,N*-donor heterocyclic bases dipyrido-[3,2-*d*:2′,3′-*f*]-quinoxaline and dipyrido-[3,2-*a*:2′,3′-*c*]phenazine were prepared by literature procedures using 1,10-phenanthroline-5,6-dione as a precursor reacted with ethylenediamine for dpq and 1,2-phenylenediamine for dppz[25-27].

The elemental analyses were done using a Thermo Finnigan Flash EA 1112 CHNS analyzer. The infrared spectra were recorded on a Bruker ALPHA FT-IR spectrometer. Electronic spectra were obtained on a Perkin Elmer Spectrum one 55 spectrophotometer. Molar conductivity measurements were carried out using a Control Dynamics (India) conductivity meter. Room temperature magnetic susceptibility data for the Gd(III) complexes were obtained from a George Associates Inc. Lewis-coil force magnetometer using $Hg[Co(NCS)_4]$ as a standard. Experimental susceptibility data were corrected for diamagnetic contributions[28]. Electrospray ionization mass spectra (ESI-MS) were recorded using Bruker Daltonics make (Esquire 300 Plus ESI Model). $^1$H NMR spectra of the ligands and the La(III) complexes were recorded at room temperature on a Bruker 400 MHz NMR spectrometer.

**Synthesis of the complexes**

Complexes **1**–**6** were prepared by following a general synthetic procedure in which a hot ethanolic solution (25 mL) of the respective phenanthroline base (B: 0.20 g phen; 0.232 g dpq; 0.283 g dppz; 1.0 mmol) was added dropwise to an ethanolic solution (25 mL) of $Ln(acac)_3.2H_2O$ (Ln = La(III), 0.453 g; Gd(III), 0.473 g; 1.0 mmol). Stirring of the reaction mixture for 30 min gave a crystalline precipitate which was isolated, washed with cold ethanol followed by cold diethyl ether, and finally dried in vacuum over $P_4O_{10}$ [Yield: ~75 %]. Diffraction quality single crystals of **4** were grown by slow evaporation of a MeOH solution of the complex. Single crystals of **5** were obtained from slow evaporation of a solution of the complex in acetonitrile/dichloromethane mixture while the single crystals of **6** were obtained by slow evaporation of a solution of the complex in chloroform/acetone mixture. The characterization data for the complexes are given below.

$[La(phen)(acac)_3]$ **(1)**: Anal. (%): Calc. for $C_{27}H_{32}N_2O_6La$: C, 52.35; H, 5.21; N, 4.52. Found: C, 52.48; H, 5.15; N, 4.40. ESI-MS in 10 % aqueous MeOH: *m/z* 536 $[M-(acac)]^+$. IR data ($cm^{-1}$): 2986w, 2911w, 1586vs, 1514vs, 1382s, 1351m, 1250s, 1195w,1100w, 1006s, 913m, 846s, 843s, 762m, 725m, 647w, 515m, 416w (vs, very strong; s, strong; m, medium; w, weak). UV-visible in DMF [$\lambda_{max}$/ nm ($\varepsilon/M^{-1}$ $cm^{-1}$)]: 351sh (3700), 280sh (5700), 266 (66300). $^1$H-NMR in DMSO-$d_6$ ($\delta$, ppm): 9.04 (dd, 2H), 8.43 (dd, 2H), 7.85 (s, 2H), 7.65 (dd, 2H), 5.2 (s, 3H), 1.72 (s, 18H).

$[La(dpq)(acac)_3]$ **(2)**: Anal. (%): Calc. for $C_{29}H_{32}N_4O_6La$: C, 51.87; H, 4.80; N, 8.34. Found: C, 52.12; H, 4.66; N, 8.31. ESI-MS in 10 % aqueous MeOH: *m/z* 572 $[M-(acac)]^+$. IR data ($cm^{-1}$): 2985w, 2912w, 1581vs, 1509vs, 1515s, 1384s, 1352m, 1249s, 1186w, 1093w, 1010s, 904m, 822m, 762m, 742m, 646w, 523m, 403w. UV-visible in DMF [$\lambda_{max}$/nm ($\varepsilon/M^{-1}$ $cm^{-1}$)]: 340 (8400), 285 (72500). $^1$H-NMR in DMSO-$d_6$ ($\delta$, ppm): 9.35 (dd, 2H), 9.2 (dd, 2H), 9.12 (s, 2H), 7.84 (dd, 2H), 5.2 (s, 3H), 1.72 (s, 18H).

$[La(dppz)(acac)_3]$ **(3)**: Anal. (%): Calc. for $C_{33}H_{34}N_4O_6La$: C, 54.93; H, 4.75; N, 7.76. Found: C, 55.10; H, 4.69; N, 7.70. ESI-MS in 10 % aqueous MeOH: *m/z* 622 $[M-(acac)]^+$. IR data ($cm^{-1}$): 2982w, 2915w, 1584vs, 1511vs, 1397s, 1355m, 1255m, 1182w, 1078w, 1006s, 914m, 825m, 758m, 653m, 611w, 524m, 408w. UV-visible in DMF [$\lambda_{max}$/nm ($\varepsilon/M^{-1}$ $cm^{-1}$)]: 380 (17000), 361 (17700), 352sh (14500), 270 (81400). $^1$H-NMR in DMSO-$d_6$ ($\delta$, ppm): 9.42 (dd, 2H), 9.15 (dd, 2H), 8.27-8.33 (m, 2H), 7.92-7.99 (m, 2H), 7.83 (dd, 2H), 5.2 (s, 3H), 1.73 (s, 18H).

$[Gd(phen)(acac)_3]$ **(4):** Anal. (%): Calc. for $C_{27}H_{32}N_2O_6Gd$: C, 50.84; H, 5.06; N, 4.39. Found: C, 51.14; H, 4.83; N, 4.28. ESI-MS in 10 % aqueous MeOH: *m/z* 536 $[M-(acac)]^+$. IR data ($cm^{-1}$): 2986w, 2915w, 1597vs, 1517vs, 1392s, 1350m, 1256s, 1185w, 1151w, 1105w, 1004s, 916m, 852s, 757m, 723s, 655m, 526m, 404w. UV-visible in DMF [$\lambda_{max}$/nm ($\varepsilon/M^{-1}$ $cm^{-1}$)]: 351sh (3700), 281 (63300), 265(67400).

$[Gd(dpq)(acac)_3]$ **(5):** Anal. (%): Calc. for $C_{29}H_{32}N_4O_6Gd$: C, 50.49; H, 4.68; N, 8.12. Found: C, 50.71; H, 4.75; N, 8.20. ESI-MS in 10 % aqueous MeOH: *m/z* 590 $[M-(acac)]^+$. IR data ($cm^{-1}$): 2983w, 2912w, 1582vs, 1511vs, 1386s, 1355m, 1251s, 1184w, 1095w, 1012s, 916m, 846w, 815w, 763m, 654m, 528m, 406w. UV-visible in DMF [$\lambda_{max}$/nm ($\varepsilon/M^{-1}$ $cm^{-1}$)]: 342 (9300), 286 (74600), 265 (60100).

$[Gd(dppz)(acac)_3]$ **(6):** Anal. (%): Calc. for $C_{33}H_{34}N_4O_6Gd$: C, 53.79; H, 4.24; N, 7.60. Found: C, 53.84; H, 4.50; N, 7.50. ESI-MS in 10 % aqueous MeOH: *m/z* 638 $[M-(acac)]^+$. IR data ($cm^{-1}$): 2983w, 2913w, 1584vs, 1515vs, 1395s, 1357m, 1258m, 1185w, 1078w, 1006s, 916m, 828m, 757m, 735s, 612w, 527m, 405w. UV-visible in DMF [$\lambda_{max}$/nm ($\varepsilon/M^{-1}$ $cm^{-1}$)]: 380 (18600), 361(18300), 351 (14500), 293sh (31000), 270 (85200).

All the complexes showed good solubility in DMF, DMSO and chlorinated solvents such as dichloromethane, chloroform and moderate solubility in methanol, ethanol and acetonitrile. The complexes were found to be stable in the solid as well as in the solution phase as seen from the molar conductivity data.

**X-ray crystallographic studies**

The crystal structures of **4** - **6** were determined by single crystal X-ray diffraction technique. Crystal mounting was done on glass fibres with epoxy cement. All geometric and intensity data were collected at room temperature using an automated Bruker SMART APEX CCD diffractometer equipped with a fine focus 1.75 kW sealed tube Mo-$K_\alpha$ X-ray source ($\lambda$ = 0.71073 Å) with increasing $\omega$ (width of 0.3° per frame) at a scan speed of 5, 5 and 7 s/frame for the complexes **4**, **5** and **6** respectively. Intensity

data, collected using $\omega$-2$\theta$ scan mode, were corrected for Lorentz – polarization effects and for absorption[29]. Structures were solved by the combination of Patterson and Fourier techniques and refined by full-matrix least-squares method using SHELX system of programs[30]. All hydrogen atoms belonging to the complexes were refined using a riding model. All the non-hydrogen atoms were refined anisotropically except one lattice $CH_2Cl_2$ molecule in complex **5** and one lattice water molecule in complex **6** that were refined isotropically. Perspective views of the molecules were obtained by ORTEP[31].

Crystallographic data and the structure refinement parameters for the complexes are given in Table 1.

**DNA binding and cleavage**

DNA binding experiments were done in Tris-HCl/NaCl buffer (5 m*M* Tris-HCl, 5 m*M* NaCl, *p*H 7.2) using DMF solution of the complexes **1**-**6**. Calf thymus (CT) DNA (ca. 350 μ*M* NP) in this buffer medium gave a ratio of UV absorbance at 260 and 280 nm of *ca.* 1.9:1 indicating that the DNA is apparently free from protein. The concentration of CT DNA was estimated from its absorption intensity at 260 nm with a known[32] molar extinction coefficient value ($\varepsilon$) of 6600 $M^{-1}$ $cm^{-1}$. The absorption titration experiments were done by following procedures as reported earlier[18]. The intrinsic equilibrium binding constant ($K_b$) and the binding site size (*s*) of the complexes **1**–**6** to CT DNA were obtained by McGhee-von Hippel (MvH) method[33] using the expression of Bard *et al.*[34] by monitoring the change of the absorption intensity of the spectral bands with increasing concentration of CT DNA. DNA melting experiments were carried out by monitoring the absorbance of CT DNA (200 μ*M*) at 260 nm at various temperatures, both in the absence and presence of the complexes (25 μ*M*). Measurements were carried out using a Cary 300 bio UV-visible spectrometer with a Cary temperature controller at an increase rate of 0.5 °C per min of the solution. Viscometric titrations were performed with a Schott Gerate AVS 310 automated viscometer that was thermostated at 37 ºC in a constant temperature bath.

Table 1 — Selected crystallographic data and structure refinement for complexes **4** - **6**

| Complex | **4** | **5**·$CH_2Cl_2$ | **6**·$2H_2O$ |
|---|---|---|---|
| Emp. formula | $C_{27}$ $H_{29}$ Gd $N_2$ $O_6$ | $C_{30}$ $H_{35}$ $Cl_2$ Gd $N_4$ $O_6$ | $C_{33}$ $H_{35}$ Gd $N_4$ $O_8$ |
| Formula wt. (g $mol^{-1}$) | 634.77 | 775.77 | 772.9 |
| Crystal system | Monoclinic | Monoclinic | Triclinic |
| Space group | $P2_1/n$ | $C2/c$ | $P$-1 |
| $a$ (Å) | 9.5027(3) | 26.6857(19) | 9.6611(5) |
| $b$ (Å) | 21.0531(7) | 18.1444(12) | 12.9183(7) |
| $c$ (Å) | 14.7621(5) | 15.1122(10) | 13.6285(7) |
| $\alpha$(°) | 90 | 90.00 | 75.067(3) |
| $\beta$(°) | 98.9970(10) | 119.759(4) | 80.083(3) |
| $\gamma$(°) | 90 | 90.00 | 86.971(3) |
| $V$ ($Å^3$) | 2916.99(17) | 6352.3(7) | 1618.84(15) |
| $Z$ | 4 | 8 | 2 |
| $T$ (K) | 293(2) | 293(2) | 293(2) |
| $\rho_{calc}$ (g $cm^{-3}$) | 1.445 | 1.622 | 1.586 |
| λ (Å) (Mo-$K_\alpha$) | 0.71073 | 0.71073 | 0.71073 |
| μ ($cm^{-1}$) | 2.312 | 2.304 | 2.105 |
| Data/ restraints/ parameters | 8879/0/325 | 9722 / 0 / 388 | 5930/0/410 |
| $F$(000) | 1268 | 3112 | 778 |
| Goodness-of-fit on $F^2$ | 1.004 | 1.013 | 1.041 |
| $R$ ($F_o$)[a], I>2$\sigma$(I) / $wR$ ($F_o$)[b] | 0.0335/0.0723 | 0.0507/0.1151 | 0.0383/0.0832 |
| $R$ (all data)/$wR$ (all data) | 0.0603/ 0.0826 | 0.1137/0.1386 | 0.0536/0.0890 |
| Largest diff. peak and hole (e $Å^{-3}$) | 0.792, -0.931 | 0.712, -0.952 | 0.858, -1.029 |

[a] $R = \Sigma||F_o|-|F_c||/\Sigma|F_o|$. [b] $wR = \{\Sigma[w(F_o^2-F_c^2)^2]/\Sigma[w(F_o)^2]\}^{1/2}$; $w = [\sigma^2(F_o)^2 + (AP)^2 + BP]^{-1}$, where $P = (F_o^2 + 2F_c^2)/3$, A = 0.0373, B = 0.5191 for **4**; A = 0.0594, B = 6.4894 for **5**.$CH_2Cl_2$ and A = 0.0435, B = 0.7465 for **6**·$2H_2O$.

The concentration of CT DNA was 150 μ*M* in NP (nucleotide pair) and the flow times were measured using an automated timer. Each sample was measured 3 times and an average flow time was calculated. Data were presented as $(\eta/\eta_0)^{1/3}$ versus [complex]/[DNA], where $\eta$ is the viscosity of DNA in the presence of the complex and $\eta_0$ is that of DNA alone. Viscosity values were calculated from the observed flow time of DNA-containing solutions ($t$) corrected for that of the buffer alone ($t_0$), $\eta = (t - t_0)/t_0$. Due corrections were made for the viscosity of DMF solvent present in the solution.

The cleavage of supercoiled (SC) pUC19 DNA (30 μ*M*, 0.2 μg, 2686 base-pairs) was studied by agarose gel electrophoresis. For photo-induced DNA cleavage studies, the reactions were carried out under illuminated conditions using UV-A light of 365 nm (6 W, model LF-206.LS of Bangalore Genei). Eppendorf vials were used for photocleavage experiments in a dark room at 25 °C using SC DNA (1 μL, 30 μ*M*) in 50 mM Tris-HCl buffer (*p*H 7.2) containing 50 m*M* NaCl and the complex (2 μL) with varied concentrations. The concentration of the complexes in DMF or the additives in buffer corresponded to the quantity in 2 μL stock solution after dilution to the 20 μL final volume using Tris-HCl buffer. The solution path length in the sample vial was ~5 mm. After light exposure, each sample was incubated for 1.0 h at 37 °C and analyzed for the photo-cleaved products using gel electrophoresis. Mechanistic studies were carried out using different additives ($NaN_3$, 0.5 m*M*; TEMP, 0.5 m*M*; DABCO, 0.5 m*M*; DMSO, 4 μL; KI, 0.5 m*M*; catalase, 4 units; SOD, 4 units) prior to the addition of the complex. For the $D_2O$ experiment, this solvent was used for dilution of the sample to 20 μL final volume. The samples after incubation in a dark chamber were added to the loading buffer containing 0.25 % bromophenol blue, 0.25 % xylene cyanol, 30 % glycerol (3 μL) and the solution was finally loaded on 1 % agarose gel containing 1.0 μg/mL ethidium bromide. Electrophoresis was carried out in a dark room for 2.0 h at 60 V in TAE (Tris-acetate EDTA) buffer. Bands were visualized in UV light and photographed. The extent of SC DNA cleavage was measured from the intensities of the bands using UVITEC Gel Documentation System. Due corrections were made for the low level of nicked circular (NC) form of DNA present in the original SC DNA sample and for the low affinity of ethidium bromide binding to SC compared to NC and linear forms of DNA[35]. The observed error in measuring the band intensities was in the range 3-5 %.

**Cytotoxicity measurements**

The photocytotoxicity of the dppz complexes and the dppz ligand was studied using 3-(4,5-dimethyl-thiazol-2-yl)-2,5-diphenyltetrazolium bromide (MTT) assay which is based on the ability of mitochondrial dehydrogenases of viable cells to damage the tetrazolium rings of MTT forming dark purple membrane impermeable crystals of formazan that could be estimated at 595 nm after solubilization in DMSO[36]. Approximately, 8000 cells of human cervical carcinoma (HeLa) were plated in 96 wells culture plate in Dulbecco's Modified Eagle Medium (DMEM) containing 10 % FBS and after 24 h of incubation at 37 °C in a $CO_2$ incubator, various concentrations of the complexes or dppz ligand dissolved in 1 % DMSO were added to the cells and incubation was continued for 4 h in dark. The medium was subsequently replaced by PBS and photo-irradiated for 15 min using UV-A light of 365 nm. After photoexposure, PBS was removed and replaced by DMEM-FBS and incubation was continued for further 24 h in dark. At the end of the incubation period, 20 μL of 5 mg $mL^{-1}$ MTT was added to each well and incubation was done for an additional 3 h. The culture medium was finally discarded and 100 μL of 10 % SDS/0.01 *M* HCl was added. The plates were then incubated at 37 °C for 6 h to dissolve the formazan crystals and the absorbances at 595 nm were recorded using a BIORAD ELISA plate reader. Cytotoxicity of the dppz ligand and the complexes was measured as the percentage ratio of the absorbance of the treated cells to the untreated controls. The $IC_{50}$ values were determined by nonlinear regression analysis using GraphPad Prism software. To determine the dark cytotoxicity of the complexes and the dppz ligand, various concentrations of the complex or dppz ligand dissolved in DMSO (1 %) were added to the HeLa cells and incubated for 24 h in dark, thereafter the media were discarded and fresh media containing 10 % FBS was added to the wells. MTT assay was then carried out as mentioned above.

## Results and Discussion

**Synthesis and characterization of La(III) complexes**

Lanthanide(III) complexes [La(B)$(acac)_3$] (**1**–**3**) and [Gd(B)$(acac)_3$] (**4**–**6**) of three phenanthroline

Table 2 — Physicochemical data and DNA binding parameters for the complexes **1–6**

| Complex | ν (C=O) ($cm^{-1}$) | $\mu_{eff}$[a] | $\Lambda_M$[b] (S $cm^2$ $M^{-1}$) | $K_b$ ($M^{-1}$) [$s$][c] | $\Delta T_m$[d] (°C) |
|---|---|---|---|---|---|
| [La(phen)(acac)$_3$] (**1**) | 1591 | – | 5 | 4.7 (±0.4) × $10^4$ [0.2] | 1.0 |
| [La(dpq)(acac)$_3$] (**2**) | 1590 | – | 7 | 3.8 (±0.2) × $10^5$ [0.4] | 2.0 |
| [La(dppz)(acac)$_3$] (**3**) | 1591 | – | 4 | 5.6 (±0.6) × $10^5$ [0.5] | 3.3 |
| [Gd(phen)(acac)$_3$] (**4**) | 1596 | 7.99 | 6 | 5.0 (±0.9) × $10^4$ [0.2] | 0.9 |
| [Gd(dpq)(acac)$_3$] (**5**) | 1591 | 7.95 | 8 | 3.6 (±0.3) × $10^5$ [0.4] | 1.9 |
| [Gd(dppz)(acac)$_3$] (**6**) | 1595 | 7.98 | 4 | 6.1 (±0.4) × $10^5$ [0.5] | 3.4 |

[a]$\mu_{eff}$ is $\mu_B$ for solid powdered samples at 298 K.
[b]$\Lambda_M$, molar conductivity in 20 % aqueous DMF at 25 °C.
[c]$K_b$, DNA binding constant [$s$, binding site size].
[d]Change in the DNA melting temp.

bases (B), viz., 1,10-phenanthroline (phen in **1**, **4**), dipyrido[3,2-*d*:2',3'-*f*]quinoxaline (dpq in **2**, **5**) and dipyrido[3,2-*a*:2',3'-*c*]phenazine (dppz in **3**, **6**), were prepared by a general synthetic procedure in which La(acac)$_3$.2H$_2$O or Gd(acac)$_3$.2H$_2$O was reacted with the corresponding phenanthroline base in ethanol (Fig. 1). The complexes were characterized from analytical and spectral data. The physicochemical data for the complexes are given in Table 2. The ESI-MS spectra of the complexes, dissolved in aqueous methanol, show prominent [M-(acac)]$^+$ peak in each case corresponding to the loss of one acac ligand from the complexes, while retaining the phenanthroline base in metal-bound form. The loss of one acac ligand could be due to the conditions used for recording the mass spectra. The molar conductivity data, however, show that the complexes are non-electrolytic in aqueous DMF retaining three acac ligands bound to the metal indicating solution stability of the complexes. The IR spectra of the complexes display a strong band around 1584 $cm^{-1}$ corresponding to the C=O stretching vibration indicating bidentate coordination of the acac ligand. The $^1$H NMR spectra of the diamagnetic La(III) complexes (**1**–**3**) dissolved in DMSO-$d_6$ show characteristic spectral features of metal-bound phenanthroline bases and acetyl-acetonate ligands. The room temperature $\mu_{eff}$ values for the Gd(III) complexes (**4**–**6**) indicate paramagnetic ($4f^7$) nature of the complexes. The electronic absorption spectra of the complexes in DMF show a ligand centered $\pi \rightarrow \pi^*$ transition at ~265 nm (Fig. 2). The dpq complexes **2** and **5** exhibit a band around 340 nm that could be due to n $\rightarrow$ $\pi^*$ transition involving the quinoxaline moiety. The dppz complexes **3** and **6** show two additional bands at 361 nm and 380 nm assignable to the n $\rightarrow$ $\pi^*$ transitions of the phenazine moiety[23]. The low-energy bands are suitable for photo-induced DNA cleavage studies using UV-A light of 365 nm.

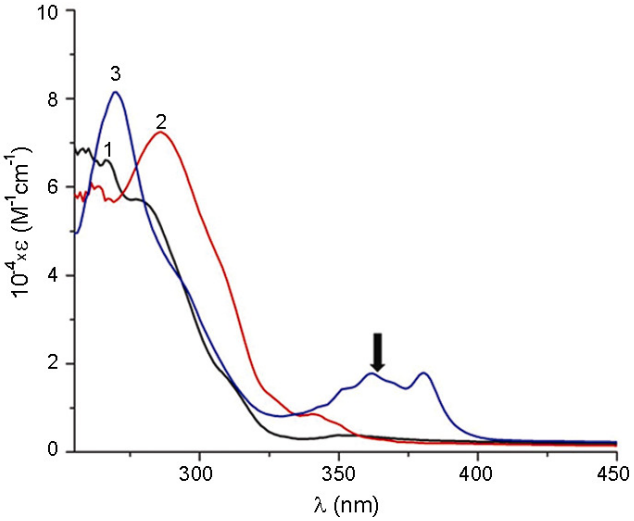


Fig. 2 – Electronic absorption spectra of the complexes **1**-**3** in DMF. [(—) comp. **1**; (—) comp. **2**; (—) comp. **3**. The wavelength (365 nm) used for the DNA photocleavage experiments is shown by an arrow].

**Crystal structures of the La(III) complexes**

The Gd(III) complexes **4** - **6** having phen, dpq and dppz ligands were structurally characterized by single crystal X-ray diffraction technique. Complex **4** crystallized in the monoclinic $P2_1/n$ space group. Complex **5** crystallized in monoclinic $C2/c$ space group. Complex **6** crystallized in the triclinic $P$-1 space group. The ORTEP views of complexes **4** - **6** are shown in Figs 3-5, respectively. Selected bond distances and bond angles are given in Tables 3 – 5. The complexes are discrete mononuclear species with the Gd(III) center in eight-coordinate $GdO_6N_2$ coordination geometry forming a distorted square

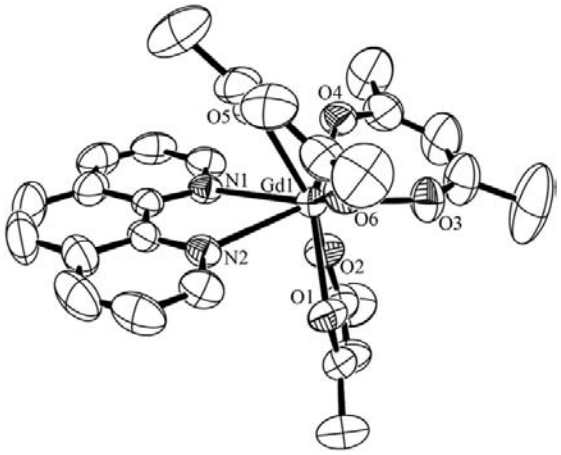


Fig. 3 – ORTEP view of [Gd(phen)(acac)$_3$] (**4**) showing atom labeling for the metal and the hetero-atoms and 50 % probability thermal ellipsoids. The hydrogen atoms are not shown for clarity.

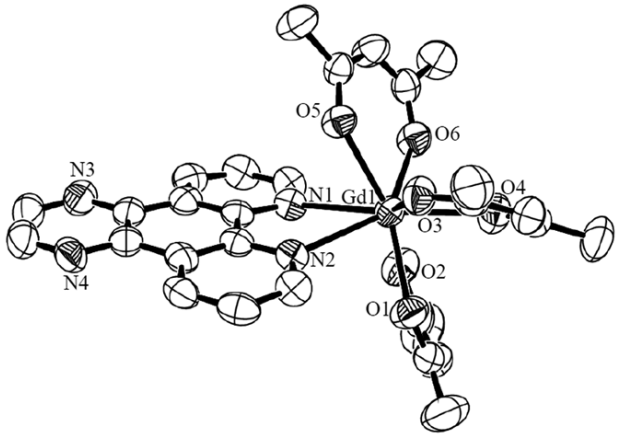


Fig. 4 – ORTEP view of the complex in [Gd(dpq)(acac)$_3$].$CH_2Cl_2$ (**5**.$CH_2Cl_2$) showing atom numbering for the metal and the hetero-atoms and thermal ellipsoids at 50 % probability. The hydrogen atoms and the solvent of crystallization are not shown for clarity.

antiprism as the coordination polyhedron with the heterocyclic bases showing bidentate *N*,*N*-coordination. All the monoanionic acetylacetonate ligands bind in a bidentate chelating fashion. The Gd-O bond distances vary in the range of 2.328(4) to 2.380(3) Å, while the Gd-N bond distances are in the range of 2.581(2) Å and 2.631(4) Å.

**DNA binding**

Absorption titration technique has been used to monitor the mode of interaction of the complexes **1–6** with CT DNA (Fig. 6). The intrinsic equilibrium DNA binding constant ($K_b$) values of the complexes along with the binding site size (*s*) are given in Table 2. The $K_b$ values of ~$10^5$ $M^{-1}$ follow the order: **3**, **6** (dppz) > **2**, **5** (dpq) > **1**, **4** (phen). The dppz complexes show higher $K_b$ values in comparison to their dpq and phen analogues possibly due to the presence of an extended aromatic moiety in dppz[37].

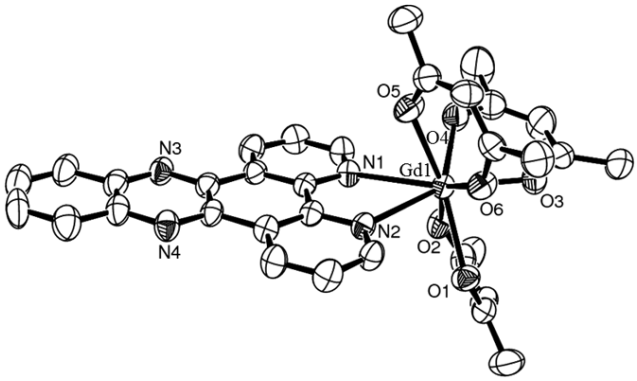


Fig. 5 – ORTEP view of the complex in [Gd(dppz)(acac)$_3$].$2H_2O$ (**6**.$2H_2O$) showing atom labeling for the metal and the hetero-atoms and 50 % probability thermal ellipsoids. The hydrogen atoms and solvents of crystallization are not shown for clarity.

Table 3 — Selected bond distances (Å) and angles (°) for [Gd(phen)(acac)$_3$] (**4**)

| Bond distances[a] (Å) | | Bond angles[a] (°) | | | | | |
|---|---|---|---|---|---|---|---|
| Gd(1)-O(1) | 2.329(2) | O(1)-Gd(1)-O(2) | 72.92(8) | O(3)-Gd(1)-O(4) | 72.77(8) | N(1)-Gd(1)-O(4) | 80.60(8) |
| Gd(1)-O(2) | 2.351(2) | O(1)-Gd(1)-O(3) | 83.86(8) | O(3)-Gd(1)-O(5) | 118.35(9) | N(1)-Gd(1)-O(5) | 72.01(8) |
| Gd(1)-O(3) | 2.368(2) | O(1)-Gd(1)-O(4) | 143.93(8) | O(3)-Gd(1)-O(6) | 77.91(8) | N(1)-Gd(1)-O(6) | 133.34(8) |
| Gd(1)-O(4) | 2.342(2) | O(1)-Gd(1)-O(5) | 140.39(8) | O(4)-Gd(1)-O(5) | 75.66(8) | N(2)-Gd(1)-O(1) | 71.15(8) |
| Gd(1)-O(5) | 2.368(2) | O(1)-Gd(1)-O(6) | 82.11(8) | O(4)-Gd(1)-O(6) | 117.92(8) | N(2)-Gd(1)-O(2) | 109.11(8) |
| Gd(1)-O(6) | 2.348(2) | O(2)-Gd(1)-O(3) | 80.72(8) | O(5)-Gd(1)-O(6) | 72.36(8) | N(2)-Gd(1)-O(3) | 148.19(8) |
| Gd(1)-N(1) | 2.581(2) | O(2)-Gd(1)-O(4) | 76.42(8) | N(1)-Gd(1)-O(1) | 108.15(7) | N(2)-Gd(1)-O(4) | 138.38(8) |
| Gd(1)-N(2) | 2.614(2) | O(2)-Gd(1)-O(5) | 138.76(8) | N(1)-Gd(1)-O(2) | 73.97(8) | N(2)-Gd(1)-O(5) | 74.69(8) |
| | | O(2)-Gd(1)-O(6) | 148.60(8) | N(1)-Gd(1)-O(3) | 146.81(8) | N(2)-Gd(1)-O(6) | 79.39(7) |
| | | | | | | N(1)-Gd(1)-N(2) | 62.83(7) |

[a]Estimated standard deviations (esd) in parentheses.

Table 4 — Selected bond distances (Å) and angles (°) for $[Gd(dpq)(acac)_3].CH_2Cl_2$ (**5**·$CH_2Cl_2$)

| Bond distances[a] (Å) | | Bond angles[a] (°) | | | | | |
|---|---|---|---|---|---|---|---|
| Gd(1)-O(1) | 2.360(4) | O(1)-Gd(1)-O(2) | 72.55(14) | O(3)-Gd(1)-O(4) | 73.90(13) | N(1)-Gd(1)-O(4) | 133.62(12) |
| Gd(1)-O(2) | 2.369(4) | O(1)-Gd(1)-O(3) | 83.73(15) | O(3)-Gd(1)-O(5) | 118.71(14) | N(1)-Gd(1)-O(5) | 71.42(13) |
| Gd(1)-O(3) | 2.338(4) | O(1)-Gd(1)-O(4) | 146.89(13) | O(3)-Gd(1)-O(6) | 76.97(14) | N(1)-Gd(1)-O(6) | 81.43(13) |
| Gd(1)-O(4) | 2.354(3) | O(1)-Gd(1)-O(5) | 138.73(13) | O(4)-Gd(1)-O(5) | 74.29(12) | N(2)-Gd(1)-O(1) | 104.64(14) |
| Gd(1)-O(5) | 2.373(3) | O(1)-Gd(1)-O(6) | 80.17(15) | O(4)-Gd(1)-O(6) | 116.87(14) | N(2)-Gd(1)-O(2) | 71.02(13) |
| Gd(1)-O(6) | 2.328(4) | O(2)-Gd(1)-O(3) | 78.27(14) | O(5)-Gd(1)-O(6) | 72.96(12) | N(2)-Gd(1)-O(3) | 143.57(14) |
| Gd(1)-N(1) | 2.631(4) | O(2)-Gd(1)-O(4) | 79.12(13) | N(1)-Gd(1)-O(1) | 74.09(13) | N(2)-Gd(1)-O(4) | 81.35(12) |
| Gd(1)-N(2) | 2.607(4) | O(2)-Gd(1)-O(5) | 141.80(12) | N(1)-Gd(1)-O(2) | 111.03(14) | N(2)-Gd(1)-O(5) | 78.21(12) |
| | | O(2)-Gd(1)-O(6) | 144.78(13) | N(1)-Gd(1)-O(3) | 151.31(14) | N(2)-Gd(1)-O(6) | 139.02(13) |
| | | | | | | N(1)-Gd(1)-N(2) | 61.89(12) |

[a]Estimated standard deviations (esd) in parentheses.

Table 5 — Selected bond distances (Å) and angles (°) for $[Gd(dppz)(acac)_3].2H_2O$ (**6**·$2H_2O$)

| Bond distances[a] (Å) | | Bond angles[a] (°) | | | | | |
|---|---|---|---|---|---|---|---|
| Gd(1)-O(1) | 2.377(3) | O(1)-Gd(1)-O(2) | 72.55(11) | O(3)-Gd(1)-O(4) | 73.01(12) | N(1)-Gd(1)-O(4) | 79.58(12) |
| Gd(1)-O(2) | 2.359(3) | O(1)-Gd(1)-O(3) | 81.84(12) | O(3)-Gd(1)-O(5) | 110.74(13) | N(1)-Gd(1)-O(5) | 73.70(11) |
| Gd(1)-O(3) | 2.344(3) | O(1)-Gd(1)-O(4) | 140.16(12) | O(3)-Gd(1)-O(6) | 75.35(12) | N(1)-Gd(1)-O(6) | 132.58(11) |
| Gd(1)-O(4) | 2.366(3) | O(1)-Gd(1)-O(5) | 145.61(12) | O(4)-Gd(1)-O(5) | 73.58(12) | N(2)-Gd(1)-O(1) | 76.66(11) |
| Gd(1)-O(5) | 2.380(3) | O(1)-Gd(1)-O(6) | 80.12(11) | O(4)-Gd(1)-O(6) | 120.88(12) | N(2)-Gd(1)-O(2) | 109.76(12) |
| Gd(1)-O(6) | 2.343(3) | O(2)-Gd(1)-O(3) | 85.36(13) | O(5)-Gd(1)-O(6) | 72.95(11) | N(2)-Gd(1)-O(3) | 148.13(12) |
| Gd(1)-N(1) | 2.607(4) | O(2)-Gd(1)-O(4) | 75.02(13) | N(1)-Gd(1)-O(1) | 112.25(12) | N(2)-Gd(1)-O(4) | 137.08(11) |
| Gd(1)-N(2) | 2.627(4) | O(2)-Gd(1)-O(5) | 138.10(12) | N(1)-Gd(1)-O(2) | 73.93(11) | N(2)-Gd(1)-O(5) | 77.12(12) |
| | | O(2)-Gd(1)-O(6) | 148.49(12) | N(1)-Gd(1)-O(3) | 149.13(12) | N(2)-Gd(1)-O(6) | 77.97(11) |
| | | | | | | N(1)-Gd(1)-N(2) | 62.37(11) |

[a]Estimated standard deviations (esd) in parentheses.

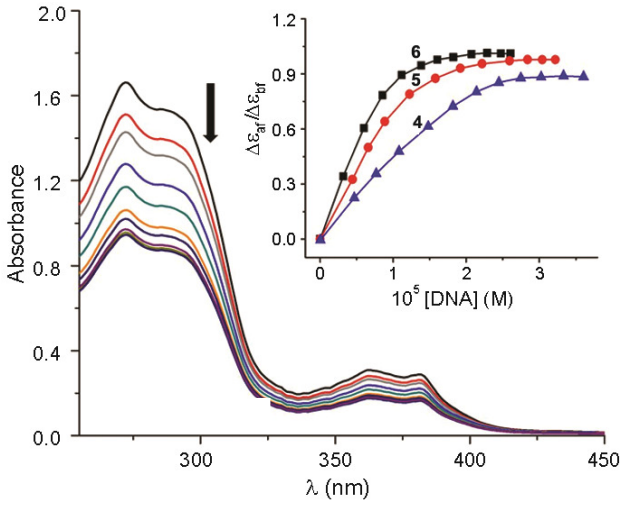


Fig. 6 – Absorption spectral traces of complex **6** in 5 m*M* Tris-HCl buffer (*p*H 7.2) on increasing the quantity of CT DNA with the inset showing the least-squares fit of $\Delta\varepsilon_{af}/\Delta\varepsilon_{bf}$ versus [DNA]. {▲, $[Gd(phen)(acac)_3]$ **(4)**; ●, $[Gd(dpq)(acac)_3]$ **(5)**; ■, $[Gd(dppz)(acac)_3]$ **(6)**}.

The *s* value, which is a fitted parameter in the MvH equation, gives a measure of the DNA interaction with the complex. A low value of *s* is typically because of aggregation of hydrophobic molecules on the surface of DNA[38]. The greater values of *s* for the dppz complexes in comparison to those for the dpq and phen complexes indicate possibility of partial intercalative mode binding of the dppz complexes to DNA.

Thermal denaturation experiments were done to gain insights into the binding of the complexes **1**–**6** to CT DNA (Fig. 7). A small positive shift of the DNA melting temperature ($\Delta T_m$) is observed upon addition of the complex to CT DNA. The low $\Delta T_m$ values suggest primarily groove binding nature of the complexes to CT DNA stabilizing the DNA double helical structure in preference to an intercalative mode of binding that normally results in large positive $\Delta T_m$ value[39,40]. The $\Delta T_m$ values for the dppz complexes are

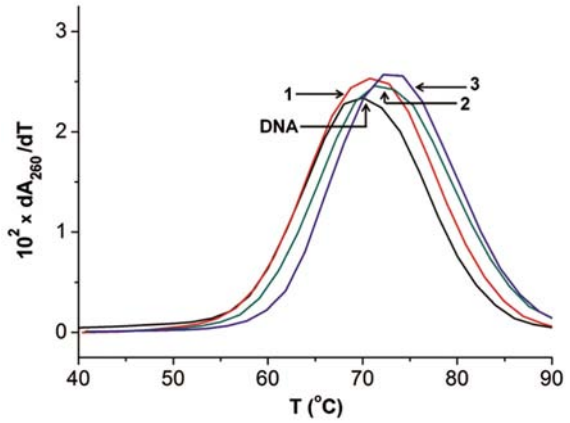


Fig. 7 – Thermal denaturation plots of 180 μ*M* CT DNA alone and on addition of the lanthanum(III) complexes **1 – 3**.

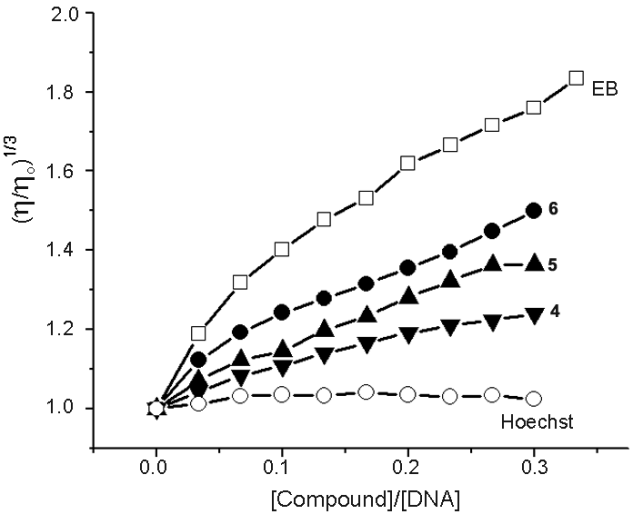


Fig. 8 – Effect of increasing the concentration of the complexes on the relative viscosities of CT-DNA (150 μ*M*) at 37.0 (± 0.1) °C in 5 m*M* Tris-HCl buffer (*p*H 7.2) containing 2.5 – 20 % DMF {▼, [Gd(phen)(acac)$_3$] (**4**); ▲, [Gd(dpq)(acac)$_3$] (**5**); ●, [Gd(dppz)(acac)$_3$] (**6**); □, ethidium bromide (EB); ○, Hoechst 33258]}.

significantly higher than those of the phen and dpq complexes. The data suggest partial intercalative mode of DNA binding for the dppz complexes. The DNA melting data for the present complexes are similar to those reported for its [$LnB_2(NO_3)_3$] analogues[18]. It is apparent from the DNA binding data of the [$LnB(acac)_3$] and [$LnB_2(NO_3)_3$] complexes that one phenanthroline base is involved in the binding to the CT DNA. The mono-phenanthroline base complexes are better suitable for photocytotoxicity study than the bis-complexes considering the dark cellular toxicity of the dppz base alone.

Viscosity measurements were carried out to examine the effect of the complexes on the specific relative viscosity of DNA (Fig. 8). Since the relative specific viscosity $\eta/\eta_0$ of DNA is a measure of the increase in contour length associated with the separation of DNA base pairs caused by intercalation, a classical DNA intercalator like ethidium bromide shows a significant increase in the viscosity of the DNA solutions ($\eta$ and $\eta_0$ are the specific viscosities of DNA in the presence and absence of the complexes, respectively). In contrast, a partial and/or non-intercalation of the ligand could result in less pronounced effect on the viscosity[41]. The groove binder Hoechst 33258 has been used as a reference compound that shows insignificant increase in viscosity. While the viscosity profile of the dppz complexes are similar to that of ethidium bromide indicating partial DNA intercalative mode of binding of the dppz complexes, the viscosity profile of the phen complex is suggestive of DNA groove binding. This observation indicates that the phen complexes possibly first interact with the DNA surface followed by groove binding[42].

**DNA photocleavage**

Photo-induced DNA cleavage activity of the complexes **1**–**6** was studied using SC pUC19 DNA (30 μ*M*, 0.2 $\mu$g) in a medium of Tris-HCl/NaCl (50 m*M*, *p*H, 7.2) buffer on irradiation with a low power monochromatic UV-A light of 365 nm. Selected DNA cleavage data are given in Table 6 and gel electrophoresis diagram is shown in Fig. 9. The phen complexes **1** and **4** are poor photocleavers of DNA in absence of any photosensitizers in these complexes. The dpq and dppz complexes with respective photoactive quinoxaline and phenazine moiety show significant photo-induced DNA cleavage activity at 365 nm. The dppz complexes **3** and **6** on photo-irradiation at 365 nm for 2 h show ~85 % cleavage of SC DNA to its NC form at a complex concentration of 2 μ*M* (lanes 8, 11 in Fig. 9). The dpq complexes **2** and **5** exhibit ~77 % cleavage of SC DNA under similar reaction conditions (lanes 7, 10 in Fig. 9). The SC DNA alone on exposure to 365 nm light does not show any significant cleavage of DNA. The ligands or the metal salts alone are inactive under similar reaction conditions. The complexes do not show any DNA cleavage in the dark thus ruling out any possibility of hydrolytic DNA cleavage. The DNA groove binding propensity of the complexes was studied using DNA minor groove binder distamycin-A and the major groove binder methyl green. Distamycin-A (50 μ*M*) alone shows ~17 %

Table 6 — Photo-induced SC DNA[a] (0.2 μg, 33.3 μ*M*) cleavage data of the complexes **1** - **6** on photo-exposure to UV-A light

| No. | React. cond.[b] | [Complex] (μ*M*) | % NC[a] |
|---|---|---|---|
| 1 | DNA control | - | 2 |
| 2 | DNA + dppz | 2 | 20 |
| 3 | DNA + [La(phen)(acac)$_3$] (**1**) | 2 | 23 |
| 4 | DNA + [La(dpq)(acac)$_3$] (**2**) | 2 | 81 |
| 5 | DNA + [La(dppz)(acac)$_3$] (**3**) | 2 | 86 |
| 6 | DNA + [Gd(phen)(acac)$_3$] (**4**) | 2 | 26 |
| 7 | DNA + [Gd(dpq)(acac)$_3$] (**5**) | 2 | 85 |
| 8 | DNA + [Gd(dppz)(acac)$_3$] (**6**) | 2 | 91 |

[a]SC and NC are supercoiled and nicked circular forms of pUC19 DNA.
[b]Wavelength: 365 nm; Ligands: 2 μ*M*; Metal salts: 2 μ*M*; Photo-exposure time: 2 h; dpq: 17 %; La(acac)$_3$.2H$_2$O: 6 %; Gd(acac)$_3$.2H$_2$O: 9 %.


Fig. 9 – Cleavage of SC pUC19 DNA (0.2 μg, 30 μ*M*) by the complexes **1**–**6** (2 μ*M*) in 50 m*M* Tris-HCl/NaCl buffer (*p*H, 7.2) containing 10 % DMF on photo-irradiation at 365 nm (6 W) for 2 h exposure. {lane 1, DNA control; lane 2, DNA + dpq (2 μ*M*); lane 3, DNA + dppz (2 μ*M*); lane 4, DNA + La(acac)$_3$.2H$_2$O (2 μ*M*); lane 5, DNA + Gd(acac)$_3$.2H$_2$O (2 μ*M*); lanes 6 - 11, DNA + complexes **1**–**6**, respectively; lane 12, DNA + distamycin-A (50 μ*M*); lane 13, DNA + distamycin-A (50 μ*M*) + **5**; lane 14, DNA + distamycin-A (50 μ*M*) + **6**; lane 15, DNA + methyl green (200 μ*M*); lane 16, DNA + methyl green (200 μ*M*) + **6**}.

cleavage of SC DNA (30 μ*M*) to its NC form at 365 nm on 2 h photoexposure. Addition of the dpq complex to distamycin-A bound SC DNA showed significant inhibition of the photocleavage activity. The dppz complex displayed no apparent inhibition in the presence of distamycin-A, but significant inhibition was observed with methyl green bound DNA. The mechanistic data suggest minor and major groove binding preferences of the dpq and dppz complexes, respectively[6,38,43].

The mechanistic aspects of the UV-A light-induced DNA cleavage reactions of **2** and **6** were studied using different additives (Fig. 10). The complexes are cleavage inactive in UV-A light of 365 nm under argon atmosphere indicating the necessity of molecular oxygen for their DNA cleavage activity. The DNA cleavage reactions under aerobic condition could follow two mechanistic pathways, viz., the type-II process forming singlet oxygen ($^1O_2$) species or a photo-redox pathway forming reactive hydroxyl radicals ($HO^\bullet$). Addition of singlet oxygen quenchers, viz., sodium azide, TEMP or DABCO to SC DNA showed partial inhibition of the photo-induced DNA cleavage activity of the complexes. Hydroxyl radical scavengers such as DMSO or catalase also showed

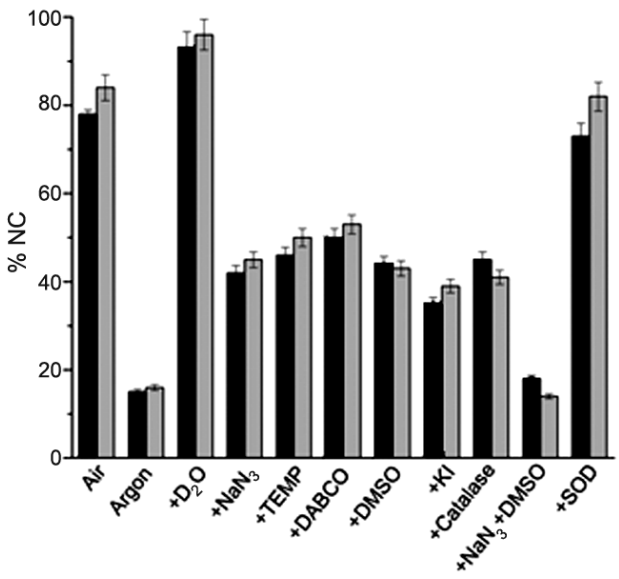


Fig. 10 – Cleavage of SC pUC19 DNA (0.2 μg, 30 μ*M*) by [La(dpq)(acac)$_3$] (**2**, black bar) and [Gd(dppz)(acac)$_3$] (**6**, light gray bar) in the presence of various additives in Tris-HCl buffer containing 10 % DMF. {Complex conc.: 2 μ*M*; exposure time for UV-A light (365 nm) expts: 2 h. Additive, conc./quantity: sodium azide, 0.5 m*M*; KI, 0.5 m*M*; TEMP, 0.5 m*M*; DABCO, 0.5 m*M*; $D_2O$, 16 μL; DMSO, 4 μL; catalase, 4 units; SOD, 4 units}.

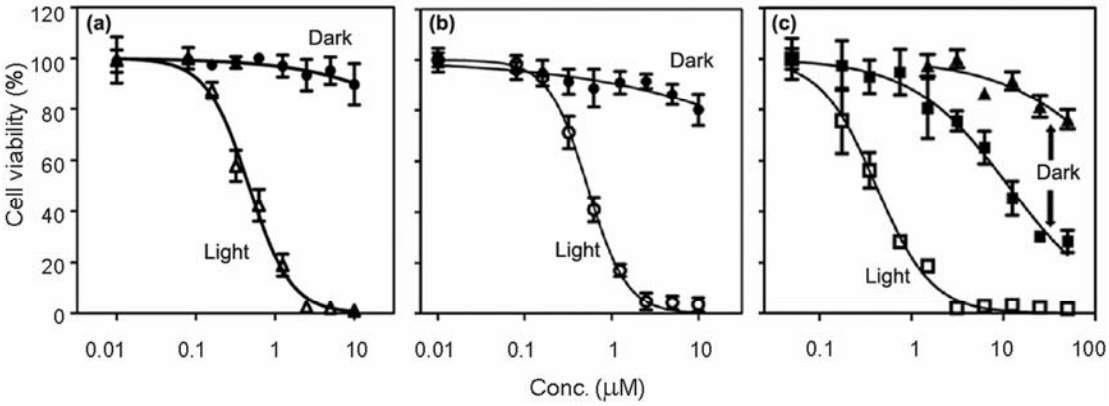


Fig. 11 – Photocytotoxicity of the complexes [La(dppz)(acac)$_3$] **(3)** (a) and [Gd(dppz)(acac)$_3$] **(6)** (b) in HeLa cells on 4 h incubation in dark followed by exposure to UV-A light (365 nm, 15 min) as determined by MTT assay. {Dark treated and photo-exposed cells in panel (a) and (b) are shown by (●) and (Δ), respectively for complex **(3)** and (●) and (○), respectively for complex **(6)**. (c) Controls: ligand dppz exposed to UV-A light (365 nm, 0.55 J cm$^{-2}$) (□); ligand dppz in dark (■); Gd(acac)$_3$.2H$_2$O in dark (▲)}.

partial inhibition of the DNA cleavage. The results suggest the involvement of both singlet oxygen and hydroxyl radicals as the reactive species. The formation of singlet oxygen was also evidenced from the reaction in $D_2O$ showing enhancement of the cleavage activity due to longer lifetime of $^1O_2$ in this medium[44,45]. While the quinoxaline/phenazine moiety could generate the singlet oxygen species in a type-II process, the formation of hydroxyl radicals could take place from electron transfer to the oxygen molecule from the photo-excited dppz base generating radical cation[46,47].

**Cell cytotoxicity**

Cellular photocytotoxicity of the dppz complexes **3** and **6** was studied in human cervical carcinoma HeLa cells by MTT assay. The complexes upon prior incubation for 4 h in dark and subsequent photo-exposure to UV-A light (365 nm) for 15 min showed a dose-dependent decrease in cell viability with an $IC_{50}$ value of 460(±50) n*M* for **3** and 530(±30) n*M* for **6** (Fig. 11). The cells unexposed to light have the $IC_{50}$ value >100 μ*M* indicating low toxicity. The dppz ligand alone shows significant dark cytotoxicity giving an $IC_{50}$ value of 11.4 μ*M* upon incubation for 24 h in dark. In UV-A light of 365 nm, the dppz base alone gives an $IC_{50}$ value of 390 n*M* upon 4 h incubation in dark followed by photo-exposure. No significant reduction in cell viability is observed upon incubation of the cells with the complex in dark for 24 h. Cisplatin is known to give an $IC_{50}$ value of 7.6 μ*M* in HeLa cells on 24 h incubation[48]. The PDT drug Photofrin® is known to have an $IC_{50}$ value of 4.3(±0.2) μ*M* on 633 nm excitation (5 *J* cm$^{-2}$) and > 41 μ*M* in dark in the same cell line[49]. The binding of the lanthanide(III) ion to dppz base is found to significantly decrease the dark toxicity of the dppz ligand, while retaining its photocytotoxicity. The lanthanide(III) ions could thus moderate the undesirable dark toxicity of photoactive organic antitumor agents for their potential applications in PDT. Interestingly, the PDT effect of the present mono-dppz complexes is found to be similar to that reported for bis-dppz complexes of Ln(III)[18]. The presence of a single dppz ligand seems to be adequate for exerting high PDT effect in this class of Ln(III) complexes.

## Conclusions

Lanthanum(III) and gadolinium(III) complexes of phenanthroline bases are prepared and their DNA binding, photo-induced DNA cleavage activity and photocytotoxicity studied. The dppz complexes show partial intercalative DNA binding propensity. The dpq and dppz complexes show significant photo-induced DNA cleavage activity at 365 nm via singlet oxygen and hydroxyl radical pathways. The dppz complexes show significant PDT effect at 365 nm giving $IC_{50}$ values at nanomolar concentration, while the complexes are non-toxic in dark with high $IC_{50}$ value of >100 μM. An important observation is that binding of the cytotoxic dppz base to the lanthanide ions significantly reduces its dark toxicity while retaining its photocytotoxicity. The mono-dppz complexes are found to show similar photocytotoxic activity as is observed for the bis-dppz analogues thus making the structurally stable mono-dppz complexes as better models for phototherapeutic studies. The results are of

importance considering that the lanthanide ions could be used as a binder to cytotoxic organic molecules having undesirable dark toxicity for their potential therapeutic applications.

## Supplementary Data

The crystallographic data have been deposited with the Cambridge Crystallographic Data Centre (CCDC reference numbers are 769201 for complex **4**, 794824 for complex **5** and 768467 for complex **6**). Copies of this information may be obtained free of charge from the Director, CCDC, 12 Union road, Cambridge, CB2 1EZ, UK (Fax: +44 1223 336 033, Email: deposit@ccdc-cam.ac.uk or www:http:// www.ccdc.cam.ac.uk).

## Acknowledgement

We thank the Department of Science and Technology (DST), Government of India, for financial support (SR/S5/MBD-02/2007). ARC thanks the DST for the J C Bose National Fellowship. AH and SS thank CSIR, New Delhi, for research fellowships.

## References

1 Crespy D, Landfester K, Schubert U S & Schiller A, *Chem Commun*, 46 (2010) 6651.
2 Farrer N J, Salassa L & Sadler P J, *Dalton Trans*, (2009) 10690.
3 Ostrowski A D & Ford P C, *Dalton Trans*, (2009) 10660.
4 Chifotides H T & Dunbar K R, *Acc Chem Res*, 38 (2005) 146.
5 Angeles-Boza A M, Chifotides H T, Aguirre J D, Chouai A, Fu P K-L, Dunbar K R & Turro C, *J Med Chem*, 49 (2006) 6841.
6 Erkkila K E, Odom D T & Barton J K, *Chem Rev*, 99 (1999) 2777.
7 Rose M J, Fry N L, Marlow R, Hinck L & Mascharak P K, *J Am Chem Soc*, 130 (2008) 8834.
8 Mackay F S, Woods J A, Heringová P, Kašpárková J, Pizarro A M, Moggach S A, Parsons S, Brabec V & Sadler P J, *Proc Natl Acad Sci USA*, 104 (2007) 20743.
9 Saha S, Majumdar R, Roy M, Dighe R R & Chakravarty A R, *Inorg Chem*, 48 (2009) 2652.
10 Sasmal P K, Saha S, Majumdar R, Dighe R R & Chakravarty A R, *Chem Commun*, (2009) 1703.
11 Bonnett R, *Chemical Aspects of Photodynamic Therapy* (Gordon & Breach, London, U K) 2000.
12 Henderson BW, Busch T M, Vaughan L A, Frawley N P, Babich D, Sosa T A, Zollo J D, Dee A S, Cooper M T, Bellnier D A, Greco W R & Oseroff A R, *Cancer Res*, 60 (2000) 525.
13 Szacilowski K , Macyk W, Drzewiecka-Matuszek A, Brindell M & Stochel G, *Chem Rev*, 105 (2005) 2647.
14 Burrows C J & Muller J G, *Chem Rev*, 98 (1998) 1109.
15 Sessler J L, Hemmi G, Mody T D, Murai T, Burrell A & Young S W, *Acc Chem Res*, 27 (1994) 43.
16 Wei W-H, Wang Z, Mizuno T, Cortez C, Fu L, Sirisawad M, Naumovski L, Magda D & Sessler J L, *Dalton Trans*, (2006) 1934.
17 Sessler J L & Miller R A, *Biochem Pharmacol*, 59 (2000) 733.
18 Hussain A, Lahiri D, Begum M S A, Saha S, Majumdar R, Dighe R R & Chakravarty A R, *Inorg Chem*, 49 (2010) 4036.
19 Frias J C, Bobba G, Cann M J, Hutchison C J & Parker D, *Org Biomol Chem*, 1 (2003) 905.
20 Werner E J, Datta A, Jocher C J & Raymond K N, *Angew Chem Int Ed*, 47 (2008) 8568.
21 Datta A & Raymond K N, *Acc Chem Res*, 42 (2009) 938.
22 Caravan P, Ellison J J, McMurry T J & Lauffer R B, *Chem Rev*, 99 (1999) 2293.
23 Toshima K, Takano R, Ozawa T & Matsumura S, *Chem Commun*, (2002) 212.
24 Perrin D D, Armarego W L F & Perrin D R, *Purification of Laboratory Chemicals* (Pergamon Press, Oxford) 1980.
25 Dickeson J E & Summers L A, *Aus J Chem*, 23 (1970) 1023.
26 Collins J G, Sleeman A D, Aldrich-Wright J R, Greguric I & Hambley T W, *Inorg Chem*, 37 (1998) 3133.
27 Amouyal E, Homsi A, Chambron J–C & Sauvage J-P, *J Chem Soc Dalton Trans*, (1990) 1841.
28 Kahn O, *Molecular Magnetism*, (VCH, Weinheim) 1993.
29 Walker N & Stuart D, *Acta Crystallogr*, A39 (1983) 158.
30 Sheldrick G M, *SHELX-97*, *Programs for Crystal Structure Solution and Refinement* (University of Göttingen, Göttingen, Germany) 1997.
31 Johnson C K, *ORTEP*, *III Report ORNL-5138* (Oak Ridge National Laboratory, Oak Ridge, TN) 1976.
32 Reichmann M E, Rice S A, Thomas C A & Doty P, *J Am Chem Soc*, 76 (1954) 3047.
33 McGhee J D & von Hippel P H, *J Mol Biol*, 86 (1974) 469.
34 Carter M T, Rodriguez M & Bard A J, *J Am Chem Soc*, 111(1989) 8901.
35 Bernadou J, Pratviel G, Bennis F, Girardet M & Meunier B, *Biochemistry*, 28 (1989) 7268.
36 Mosmann T, *J Immunol Methods*, 65 (1983) 55.
37 Phillips T, Haq I, Meijer A J H M, Adams H, Soutar I, Swanson L, Sykes M. J & Thomas J A, *Biochemistry*, 43(2004) 13657.
38 Angeles-Boza A M, Bradely P M, Fu P K-L, Wicke S E, Bacsa J, Dunbar K R & Turro C, *Inorg Chem*, 43 (2004) 8510.
39 An Y, Liu S-D, Deng S-Y, Ji L-N & Mao Z-W, *J Inorg Biochem*, 100 (2006) 1586.
40 Gunther L E & Yong A S, *J Am Chem Soc*, 90 (1968) 7323.
41 Veal J M & Rill R L, *Biochemistry*, 30 (1991) 1132.
42 Pellegrini P P & Aldrich-Wright J R, *Dalton Trans*, (2003) 176.
43 Delaney S, Pascaly M, Bhattacharya P K, Han K & Barton J K *Inorg Chem*, 41(2002) 1966.
44 Khan A U, *J Phys Chem*, 80 (1976) 2219.
45 Merkel P B & Kearns D R, *J Am Chem Soc*, 94 (1972) 1029.
46 Tanaka M, Ohkubo K & Fukuzumi S, *J Phys Chem A*,110 (2006) 11214.
47 Cunningham M L, Johnson J S, Giovanazzi S M & Peak M J, *Photochem Photobiol*, 42 (1985) 125.
48 Kang H C, Kim I-J, Park H-W, Jang S-G, Ahn S-A, Yoon S N, Chang H-J, Yoo B C & Park J-G, *Cancer Lett*, 247 (2007) 40.
49 Delaey E, Van Laar F, De Vos D, Kamuhabwa A, Jacobs P & De Witte P, *J Photochem Photobiol B*, 55 (2000) 27.